Binding and Location of Dipyridamole Derivatives in Micelles: the Role of Drug Molecular Structure and Charge

Iouri E.Borissevitch[a+], Christiane P.F.Borges[a++], Galina P.Borissevitch[a+++], Victor E.Yushmanov[a+], Sonia R.W.Louro[b] and Marcel Tabak[a]

[a] Instituto de Química de São Carlos, Universidade de São Paulo, C.P 780, 13560–970, São Carlos, SP, Brasil
[b] Departamento de Física, Pontifícia Universidade Católica do Rio de Janeiro, 22452.970 RJ, Brasil

Z. Naturforsch. **51 c,** 578–590 (1996); received March 28/May 31, 1996

Dipyridamole and Derivatives, Micelle, Drug Location, Absorption, Fluorescence, NMR

Binding and localization of the vasodilator and antitumor drug coactivator dipyridamole (DIP) and of its three derivatives, RA14, RA47 and RA25 (DIPD), to cationic (cetyltrimethylammonium chloride), anionic (sodium dodecylsulfate), zwitterionic (N-hexadecyl-N,N-dimethyl-3-ammonio-1-propanesulfonate), and neutral (*t*-octylphenoxypolyethoxyethanol) micelles was studied using fluorescence, optical absorption and ^{1}H NMR spectroscopy. The analysis of NMR, optical absorption and fluorescence data indicates that the depth of localization of the drugs in the micelles from the surface decreased in the order DIP > RA14 > RA47 > RA25. The binding constants for the neutral drug forms change in the same order in the range of 1400–3100 M^{-1} for DIP to 80–300 M^{-1} for RA25. This order is identical with the reported biological activity of DIPD. For the protonated drugs in zwitterionic or neutral micelles the binding constants are reduced by a factor of 20–75.

Introduction

Dipyridamole, (DIP), 2,6-bis(diethanolamino)-4,8-dipiperidinopyrimido[5,4-d] pyrimidine, is well known as a coronary vasodilator and has been used in clinics for many years (Marshall and Parrat, 1973; Marchandt *et al.*, 1984). Recently it has been shown that it can also act as a coactivator of a number of antitumor compounds (Batisda *et al.*, 1985; Asoh *et al.*, 1989; Ford and Hait, 1990; Zhen *et al.*, 1992). In many cases the tumor cell resistance to certain classes of drugs in cancer chemotherapy is due to the overexpression of P-glycoprotein (P-gp), which is a transmembrane nonspecific ATP-dependent efflux pump of lipophilic substances. According to (Shalinsky *et al.*, 1990, 1993) and (Chen *et al.*, 1993) DIP and its derivatives (DIPD) can inhibit the P-gp pump function. The affinity of DIP to lipid phase is confirmed by the fact that it is an inhibitor of the membrane peroxidation (Iuliano *et al.*, 1989, 1992, 1995; Hiramatsu *et al.*, 1992). From the other hand it was shown that it binds effectively with micelles (Tabak and Borissevitch, 1992; Borges *et al.*, 1995; Borissevitch *et al.*, 1995) and phospholipid monolayers (Borissevitch *et al.*, 1996). These data suggest that the effects of DIP and its derivatives could be mediated by the membranes.

The biological activity of DIPD depends upon the nature of the substituents in different positions of the molecule. This was demonstrated by both the DIPD-induced inhibition of adenosine and phosphate transport in red blood cells (Von Gerlach *et al.*, 1965) and the restoration of the sensitivity of the drug-resistant cells to adriamycin (Ramu and Ramu, 1989). The structure of DIPD molecules can influence their affinity to membrane lipid phase and position in the membrane. Therefore, we considered a study on the effect of DIPD side substituents on their interaction with membrane models.

Notwithstanding their simplicity, micelles have been often used as a model of a biological membrane, in particular, when a problem of location of foreign molecules (e. g. drugs) in an organized

[+] On leave the Institute of Chemical Physics, Russian Academy of Sciences, Moscow, Russia.
[++] Present address: Universidade Federal de Ponta Grossa, Ponta Grossa, PR, Brasil.
[+++] On leave from the Lomonossov State University, Moscow, Russia.

Reprint requests to Dr. Tabak.
Fax: 55-162-749163.

0939–5075/96/0700–0578 $ 06.00

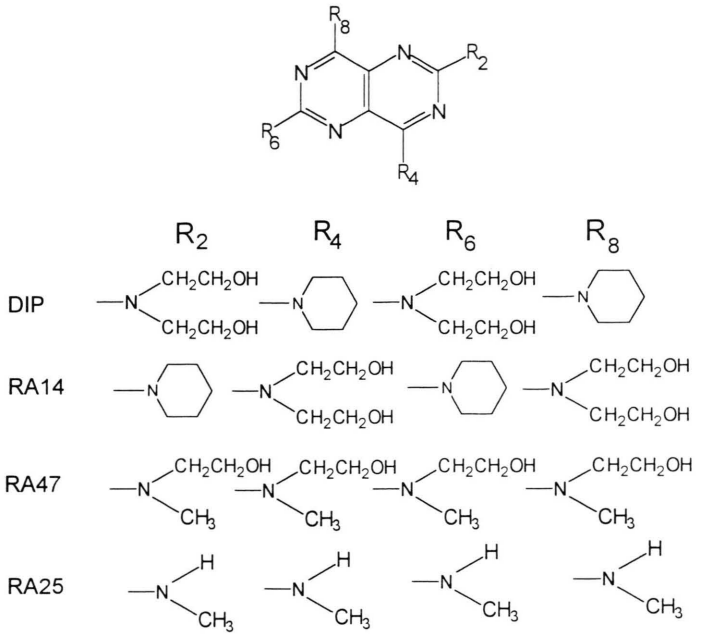

Fig. 1. Structural formulae of dipyridamole and its derivatives.

system of amphipathic substances has been put forward (Tanford, 1973; Louro *et al.*, 1994).

In previous studies, we have shown that DIP in micelles is localized in the region that separates their polar and nonpolar parts (Borissevitch *et al.*, 1995). Similar results were obtained in experiments with phospholipid Langmuir monolayers (Borissevitch *et al.*, 1996) making it reasonable to assume that DIP molecules may have similar location in biological membranes.

In the present work, we determined the binding characteristics and the location sites of three DIPD (Fig. 1) in cationic cetyltrimethylammonium chloride (CTAC), anionic sodium dodecyl sulfate (SDS), zwitterionic N-hexadecyl-N,N-dimethyl-3-ammonio-1-propanesulfonate (HPS) and neutral t-octylphenoxypolyethoxyethanol (TRITON X-100) micelles using absorption, fluorescence emission and proton NMR spectroscopies. The dependence of the binding characteristics on the structure of the substituents was considered in comparison with DIP taking into account the ionization state of the drug molecules and the micellar charge. Fluorescence quenching with nitroxide radicals 2,2,6,6-tetramethylpiperidine-1-oxyl (TEMPO) and 2,2,6,6-tetramethylpiperidine-4-hydroxy-1-oxyl(TEMPOL) was also used as an additional tool. Since all DIPD have pK values for nitrogen protonation in the physiological range (Borissevitch and Tabak, 1992; Borges and Tabak, 1994), properties of both protonated and neutral drugs were compared.

Material and methods

DIP, HPS and TRITON X-100 were purchased from Sigma, SDS from Bio-Rad, CTAC was from Herga and recrystallized twice from methanol-acetone (1:4) and dried under vacuum. DIPDs were a kind gift from Dr. Karl Thomae GmbH, Biberach am Riss. TEMPOL was produced by oxidation of its precursor obtained from Aldrich, TEMPO and solvents D_2O and $CDCl_3$ were purchased from Aldrich (USA). All other reagents were analytical grade and used as supplied. H_2O was distilled and deionized. The experiments at fixed pHs were made in acetate (pH 2.0, 3.0 and 5.0), phosphate (pH 7.0) and borate (pH 9.0) buffers (all 0.02 M). The pH titrations were carried out in water using HCl or NaOH concentrated stock solutions.

In fluorescence measurements, the DIPD concentration was in the range from 5 to 10 μM so that the optical density at the excitation wavelength (maximum of absorption) was less than 0.1. The association constants (K_b) of drugs to micelles

were determined by fluorimetric titrations at a fixed concentration of the drug and with the addition of small aliquots of concentrated surfactant solutions directly to the cuvette. Data were analyzed as described previously (Tabak and Borissevitch, 1992; Borges *et al.*, 1995). Each K_b value is an average of five independent experiments.

In quenching experiments, small aliquots of stock solutions of nitroxide radicals in ethanol (TEMPO, 0.32 M) and in water (TEMPOL, 0.18 M) were added to the cuvette, and the fluorescence intensity at the maximum emission wavelength was monitored. Data were treated as Stern-Volmer plots. The bimolecular quenching constants were determined from the relationship $K_{sv} = k_q * \tau_{fl}$, where K_{sv} is the slope of the Stern-Volmer plot, k_q is the bimolecular constant and τ_{fl} is the fluorescence lifetime in the absence of the quencher.

Fluorescence quantum yields (φ_{fl}) for different solutions of DIPD were obtained with fluorescein in 0.1 N NaOH (φ_{fl} = 0.92) as a standard. The following concentrations of micelles were used in the quenching experiments and to measure the absorption and emission spectra of the bound DIPD forms: from 0.10 to 0.50 M of CTAC, from 0.05 to 0.30 M of HPS, from 0.10 to 0.30 M of SDS and from 0.05 to 0.1 M of TRITON X-100.

In NMR measurements, the DIPD concentration was in the range of 1 to 5 mM in D_2O, $CDCl_3$ and in aqueous solutions of SDS and CTAC, and less than 100 μM in CCl_4 (saturated solution). The millimolar concentration of DIPD in D_2O was reached in the acidic medium (pH 2.0), and after the addition of micelles the pH was adjusted up to the desired value (pH 7.0 for CTAC and pH 5.0 and 9.0 for SDS).

Fluorescence measurements were performed on a JASCO FP-777 spectrofluorimeter, absorption was monitored on a Hitachi U-2000 spectrophotometer, fluorescence lifetimes were measured using a nanosecond lifetime system from PTI, model LS-1, proton NMR spectra were run on a Bruker AC-200 spectrometer. The pH values were measured by a Corning 130 pH meter equipped with a glass Ag/AgCl semimicro combination electrode. All measurements were made at room temperature.

Results and discussion

Absorption and fluorescence spectra of DIPD

The optical absorption (320–500 nm) and fluorescence emission (380–600 nm) spectra of DIPD (Tables I, II) are characterized by the bands due to the $\pi \rightarrow \pi^*$ and $\pi \leftarrow \pi^*$ transitions in the heteroaromatic cycle, respectively (Borissevitch and Tabak, 1992; Borges and Tabak, 1994).

Both absorption and fluorescence spectra of DIPD are insensitive to the polarity of the solvents in the range of dielectric constants ε from ≈33 to ≈8. For each DIPD the spectra practically coincide in the row of the alcohols from methanol (ε=33.6) to 1-decanol (ε=8.1) and in acetone (ε= 20.7). However, outside the mentioned ε range the maximum positions and the band shapes in both spectra are changed. Thus, a difference is observed for chloroform (ε=4.8), and it is even larger for hexane (ε=1.9) and CCl_4 (ε=2.2) or in glycerol (ε= 42.5) and water (ε=80.4) (Tables I, II; Fig.2, 3a).

The DIPD molecules have eight nitrogen atoms that can be protonated. This multiple protonation is confirmed by the dramatic increase of DIPD solubility upon acidification. Indeed, the solubility

Table I. Spectral characteristics of neutral DIPD in homogeneous solutions.

Solvent	ε	DIP		RA14		RA47		RA25	
		λ^{abs}_{max} [nm]	λ^{fl}_{max} [nm]	λ^{abs}_{max} [nm]	λ^{fl}_{max} [nm]	λ^{abs}_{max} [nm]	λ^{fl}_{max} [nm]	λ^{abs}_{max} [nm]	λ^{fl}_{max} [nm]
Glycerol	42.5	411	484	413	504	407	487	376	450
Methanol	33.6	410	476	410	490	406	479	374	444
Ethanol	24.3	410	478	410	490	407	478	374	445
Acetone	20.7	411	476	410	488	407	478	373	443
1-Decanol	8.1	411	476	411	488	407	478	375	444
Chloroform	4.8	412	478	410	496	409	482	372	440
Hexane	1.9	414	469	414	482	–	–	366	424

Table II. DIPD spectral characteristics in aqueous and micellar solutions.

DIPD	Micelles	Neutral form				Protonated form			
		λ^{abs}_{max} [nm]	λ^{fl}_{max} [nm]	[a]φ_{fl} [%]	[b]τ_{fl} [nsec]	λ^{abs}_{max} [nm]	λ^{fl}_{max} [nm]	[a]φ_{fl} [%]	[b]τ_{fl} [nsec]
DIP	H_2O	418	500	99	17.7	407	500	12	8.6
	CTA	411	478	100	17.2	405	484	16	11.2
	TRITON	411	478	100	–	402	485	12	–
	HPS	411	478	100	16.7	402	486	10	6.2
	SDS	411	478	100	17.1	404	487	12	2.7
RA14	H_2O	405	512	70	19.5	403	512	2	41.4
	CTAC	410	496	89	20.5	–	–	8	6.1
	TRITON	411	497	91	–	400	499	7	–
	HPS	410	496	91	21.0	400	498	6	5.8
	SDS	409	504	100	19.3	408	502	7	4.7
RA47	H_2O	407	496	76	18.1	392	498	4	–
	CTAC	408	482	92	17.7	–	–	5	2.7
	TRITON	408	482	96	–	–	–	5	–
	HPS	408	482	97	18.2	–	–	5	2.2
	SDS	408	482	100	18.0	402	484	11	2.9
RA25	H_2O	372	451	100	15.0	–	–	57	9.6
	CTAC	375	450	63	13.9	–	–	50	–
	TRITON	376	450	76	–	–	–	60	–
	HPS	375	450	77	16.1	–	–	60	11.4
	SDS	373	450	100	15.6	–	–	87	15.6

[a] The accuracy of determination is 20%; [b] the accuracy of determination is 10%.

of DIP is: 15 μM at pH 7.0, 170 μM at pH 5.0, 7 mM at pH 3.0 and 160 mM at pH 1.0, respectively. The protonation changes the spectral properties of DIPD. However, as a rule, it is just the first protonation that reduces φ_{fl}, τ_{fl} and changes the absorption and fluorescence spectra (Table II). It is practically impossible to reveal other protonation steps from optical measurements. The only exception is RA25, which has two jumps in the pH dependences of absorption and fluorescence intensities. The pK_a values of the first DIPD protonation are presented in Table III.

The absorption and fluorescence spectra and the pK_a values of DIPD in aqueous solutions change in the presence of micelles (Tables II, III). These changes indicate the binding of DIPD molecules to the micelles. Moreover, the data on fluorescence quenching presented later also demonstrate the binding.

Two regions are usually distinguished in the micelle structure (Tanford, 1973; Wennerström and Lindman, 1979): (a) the micelle core composed of the hydrophobic tails and (b) the polar sphere composed of the heads of the amphipathic molecules. The region (a) does not contain water and is characterized by a low dielectric constant (ε=2–4). The region (b) contains both water molecules

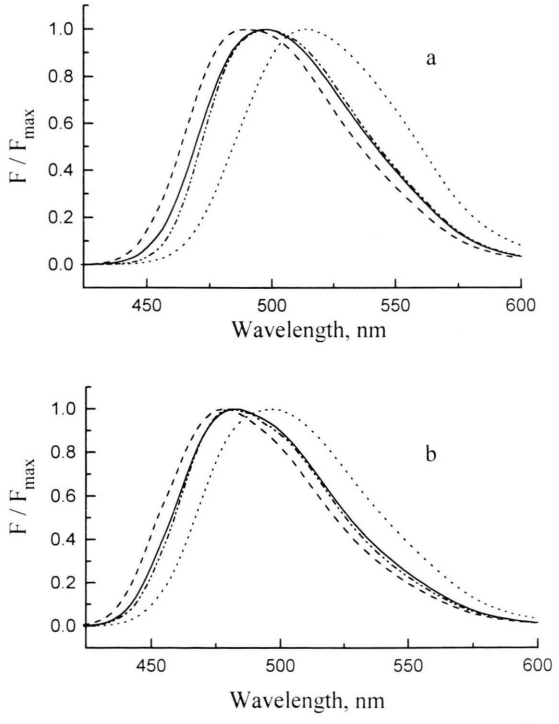

Fig. 2. Emission fluorescence spectra of RA14 (a) and RA47 (b) in H_2O (·····) and CTAC micellar solution (——) at pH 7.0, $CHCl_3$ (-·-·-·-) and EtOH (- - - -). Concentration of RA14 and RA47 is 15μM, concentration of CTAC is 100 mM. Excitation at 405 nm.

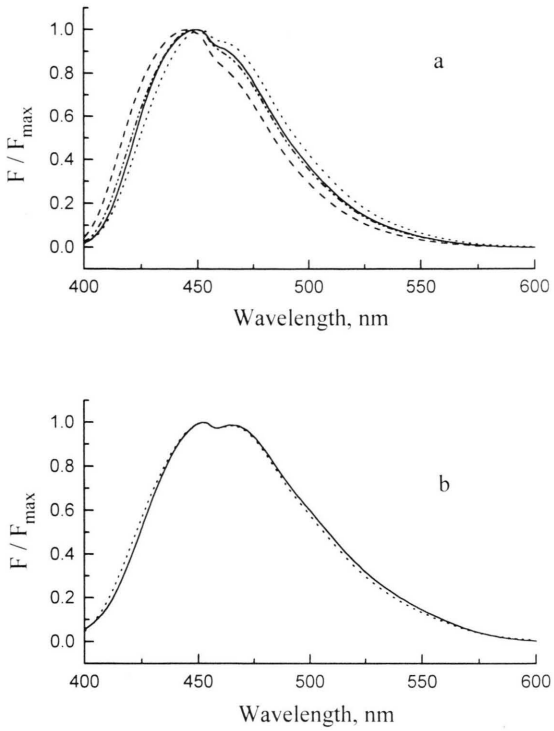

Fig. 3. Emission fluorescence spectra of RA25: a) in H_2O (·····) and CTAC micellar solution (——) at pH 7.0, EtOH:H_2O = 3:2 (-·-·-·-) and EtOH (- - - -); b) in H_2O at pH 2.0 (·····) and SDS micellar solution (——) at pH 3.0. Concentration of RA25 is 15μM, concentration of CTAC and SDS is 100 mM. Excitation at 375 nm.

and the counterions necessary for the stabilization of its structure. The water content in this region is relatively low (Wennerström and Lindman, 1979). The dielectric constant of the region (b) is higher than that of the region (a). Actually, there exists one more region between the micelle surface and the bulk water, which consists of water molecules structured due to the interaction with the polar surfactant headgroups (Fernández and Fromherz, 1977; Kaneshina *et al.*, 1984; Thomas, 1980; Drummond *et al.*, 1988; Tocanne and Teissié, 1990). The properties of this region differ from those of the bulk solvent and from regions (a) and (b). Recent theoretical and model data on the hydration of phospholipid mono- and bilayers postulate, in agreement with the experimental results, the existence of several layers of structured water close to the polar phospholipid headgroups. These layers provide the means for the existence of a very steep gradient of ε in the interface region, decreasing from ε=80 in the bulk to a value of about ε=5–7 in the polar region over a distance about 10–15 Å with average ε values in the range of 30–40 (Tocanne and Teissié, 1990; Alper *et al.*, 1993; Oliveira *et al.*, 1989; Taylor *et al.*, 1990). This model can also be applied to describe the micelle interface ((Fernández and Fromherz, 1977; Kaneshina *et al.*, 1984; Thomas, 1980; Drummond *et al.*, 1988; Tocanne and Teissié, 1990). Hence, we can distinguish the region (c), located between the micelle surface and the bulk solution, which consists of the structured water molecules and is characterized by a steep ε gradient perpendicular to the micelle surface.

The linear sizes of the DIPD molecules (≈7Å) are comparable or less than the sizes of any of these three regions. In principle, DIPD bound to the micelles could be localized in any of these regions or span more than one region. It is worth considering here the symmetry of the DIPD molecules. The planar symmetry of the heteroaromatic cycle, which is common to all derivatives, and the symmetrical location of the side substituents suggest that the neutral drug molecule binds to the micelle with its heterocycle parallel to the micelle

Table III. Values of pK_a, ΔpK_a and electrostatic potential in micellar solutions.

DIPD	Solution	pK_a	ΔpK_a	[a]ΔpK_e	[b]$e\Psi\times10^{-3}$ (eV)
DIP	H_2O	5.8	–	–	–
	CTAC	3.5	−2.3	−0.9	49.9
	HPS	4.3	−1.5	−0.1	5.5
	TRITON	4.4	−1.4	0	0
	SDS	7.3	1.5	2.9	−160.8
RA14	H_2O	5.8	–	–	–
	CTAC	3.7	−2.1	−0.9	49.9
	HPS	4.4	−1.4	−0.2	11.0
	TRITON	4.6	−1.2	0	0
	SDS	7.6	1.8	3.0	−166.3
RA47	H_2O	6.4	–	–	–
	CTAC	4.6	−1.8	−0.8	44.4
	HPS	5.1	−1.3	−0.3	16.5
	TRITON	5.4	−1.0	0	0
	SDS	7.7	1.3	2.3	−127.5
RA25	H_2O	5.2	–	–	–
	CTAC	4.9	−0.3	−0.2	11.0
	HPS	4.9	−0.3	−0.2	11.0
	TRITON	5.1	−0.1	0	0
	SDS	8.7	3.5	3.6	−199.6

[a] From the expression $\Delta pK_e = \Delta pK_a - \Delta pK_i$; $\Delta pK_i = \Delta pK_a(\text{Triton}) = \Delta pK_a(\text{HPS})$; [b] from the expression $e\Psi = -2.3\,kT\,\Delta pK_e$.

surface since for the neutral form of the drug there is no reason to break this symmetry. The difference in the properties of the substituents would be responsible for a deeper or shallower location of the DIPD molecules in the gradient of polarity, which is perpendicular to the micelle surface.

The spectral changes for RA14 and RA47 in the presence of the micelles in the solution are similar to those for DIP (Borissevitch *et al.*, 1995; Borges *et al.*, 1995). The results for RA25, which are different, are presented separately.

RA14 and RA47

The absorption and fluorescence spectra of RA14 and RA47 in all types of micelles are nearly the same as in chloroform, and differ from those in solvents with higher or lower dielectric constants (Tables I, II; Fig.2). Since these spectra are due to the $\pi^* \Leftrightarrow \pi$ transitions in the heteroaromatic cycle, this similarity indicates that their cycles are in an environment with $\varepsilon \approx 5$, i.e. in the region (b). This is in agreement with the data on the preferential location of certain aromatic compounds in the polar headgroup region of micelles (Ganesh *et al.*, 1982). The DIPD affinity to the environment with moderate polarity is also confirmed by the data on their solubility: it is higher in solvents with moderate polarity (chloroform, acetone, alcohols) than in nonpolar (hexane) or highly polar (water, glycerol) solvents.

RA25

The absorption spectra of neutral RA25 are similar in all the solvents used (except for hexane) and in all types of micelles (Tables I, II); its fluorescence spectra in micelles are close to those in a water-ethanol mixture H_2O:EtOH = 2:3 (Fig.3a). This indicates that the neutral RA25 molecules are located in a region where $34<\varepsilon<80$, in other words, in the region (c). For the protonated RA25 in SDS its fluorescence spectra are close to those in water solutions, however, the pH values in the presence of micelles are higher (Fig.3b). This suggests that the heterocycle of protonated RA25 is localized near the negatively charged micelle surface in the region enriched with protons and has the water environment. Hence, it is probably localized in the region (c), as well.

Association constants and pK_a shifts of DIPD in micelles

The K_b values for binding of neutral and protonated DIPD to micelles were estimated by titration

Table IV. Solubility, biological activity and characteristics of binding of neutral and protonated (H^+) DIPD to micelles.

DIPD	[a]Solubility $\times 10^{-5}$ M	[b]Activity adenosine	[c]Activity phosphate	Solution	[d]K_b M^{-1}	[d]$K_b(H^+)$ M^{-1}	$K_b/K_b(H^+)$
DIP	1.5 ± 0.5	+++++	+++++	CTAC	3100	11	281.8
				TRITON	1400	25	56.0
				HPS	1600	25	64.0
				SDS	1800	>3000	<0.6
RA14	2.6 ± 1.0	+++++	+++++	CTAC	2200	2.5	880.0
				TRITON	1300	–	–
				HPS	1100	15	73.3
				SDS	1500	>2000	<0.7
RA47	11.0 ± 3.0	++++	+++	CTAC	450	<5	<90.0
				TRITON	200	–	–
				HPS	150	7.5	20.0
				SDS	500	–	–
RA25	26.0 ± 6.0	0	0	CTAC	130	<5	>26.0
				TRITON	80	–	–
				HPS	100	<5	>20.0
				SDS	300	–	–

[a] Solubility in 0.02 M phosphate buffer at pH 7.0; [b] determination from the inhibition of the adenosine transport in red blood cell (Von Gerlach *et al.*, 1965); [c] determination from the inhibition of the phosphate transport in red blood cell (Von Gerlach *et al.*, 1965); [d] accuracy of determination is 20%.

of a drug solution at a fixed concentration at a given pH with variable amounts of the surfactant. The appropriate pH to perform the titration was chosen based on the pK_a values for the drugs in the micelles (Table III). For CTAC, HPS and TRITON X-100 they were 7.0 for all DIPD, 2.0 for RA14 and RA47 and 3.0 for RA25, while for SDS the values of 5.0 and 9.0 were used for all DIPD. The K_b values decrease following the sequence DIP>RA14>RA47>RA25 for the neutral forms of DIPD in all types of micelles (Table IV). This sequence is opposite to that of the water solubilities of DIPD neutral forms. Since all DIPD molecules share a common central heterocycle, the variation in their water solubility is due to the difference in structure of side substituents, which determine the above sequence of relative DIPD hydrophobicity and affinity to micelles. For the protonated forms the sequence is not so clear, since the experimental values of K_b for RA47 and RA25 in CTAC and HPS micelles have a high dispersion and cannot be determined with sufficient accuracy. For SDS the binding of protonated DIPD is already complete at SDS concentrations just slightly above the critical micelle concentration, and the K_b also can not be determined accurately. However, it is possible to assert that for all types of DIPD the protonation reduces dramatically the K_b values for TRITON X-100, HPS and CTAC micelles and increases them for SDS ones.

The K_b values for DIPD change at protonation due to two factors: (1) the increase in polarity upon protonation, which reduces the affinity to the hydrophobic micelle interior. This effect is clearly observed in neutral and zwiterionic micelles, where the protonation reduces the K_b values by factors from 20 to 75 (Table IV); (2) the electrostatic interaction between the charged micelle surface and the positive charge of the protonated DIPD molecule. In cationic CTAC micelles the electrostatic repulsion reduces and in anionic SDS the attraction increases the K_b of protonated DIPD by several orders of magnitude as compared with neutral and zwiterionic micelles.

In order to determine the apparent pK_a shift (ΔpK_a) due to the interaction of the drug with the surfactants, experiments were performed at relatively high concentrations of the surfactant in the solution ensuring almost complete binding of DIPD to micelles.

The addition of neutral, zwitterionic and positively charged surfactants induces a negative pK shift of DIPD, while for the negatively charged SDS this shift is positive (Table III). The observed ΔpK_a includes two terms (Drummond *et al.*, 1988; Davies and Rideal, 1961; Lee, 1978; Rooney *et al.*, 1983; Louro *et al.*, 1994):

$$\Delta pK_a = \Delta pK_i + \Delta pK_e$$

where ΔpK_i is the intrinsic shift due to the new environment of DIPD, which has different physical and chemical characteristics, ΔpK_e is the electrostatic shift due to the difference in the bulk H^+ concentration and the local H^+ concentration near the micelle surface caused by the electrostatic interaction between H^+ and the charged micelle surface.

For neutral micelles, ΔpK_e equals zero and ΔpK_a=ΔpK_i. The absolute values of ΔpK_i in the presence of TRITON X-100 follow the sequence DIP>RA14>RA47>RA25≈0. The ΔpK_i values for DIP, RA14 and RA47 are high, which means that their environment changes strongly upon binding, and the difference between the K_b values for the neutral and charged drug forms is large even in the absence of a net micelle charge. The measured difference in the ΔpK_i values for these three DIPD, though rather small, indicates, however, the difference in their position within the micelle, DIP being located deeper and RA47 shallower as compared with RA14. The small ΔpK_i value for RA25 means that the characteristics of its environment in micelles are close to those in the bulk.

Assuming that the ΔpK_i is the same for all types of micelles, we can derive ΔpK_e for the positively and negatively charged micelles as $\Delta pK_e = \Delta pK_a - \Delta pK_i$ (Table III). The H^+ concentration near the micelle surface is given by the Boltzmann equation

$$[H^+] = [H^+]_o \exp(-e\Psi / 2.3\,kT)$$

where $[H^+]_o$ is the bulk proton concentration, Ψ is the electrostatic potential in the aqueous phase adjacent to the micelle surface and e is the elementary charge. The potentials $e\Psi$ (in energy units) were calculated as

$$e\psi = -2.3\,kT\,\Delta pK_e$$

and are also shown in Table II.

Table V. DIPD bimolecular quenching constants $k_q \times 10^{-10}$ ($M^{-1}sec^{-1}$) by TEMPO and *TEMPOL**.

	EtOH (TEMPO) *H_2O (TEMPOL)*	CTAC H^+		HPS H^+		SDS H^+	
DIP	0.69 *(0.72)*	2.4 *(0.79)*	1.5 *(0.63)*	1.7 *(0.73)*	1.3 *(0.48)*	2.6 *(1.9)*	1.7 *(0.78)*
RA14	– *(0.59)*	–	1.5 *(0.65)*	1.9 *(0.64)*	1.4 *(0.43)*	1.2 *(0.47)*	3.0 *(0.90)*
RA47	– *(0.64)*	– –	1.7 *(0.90)*	– –	1.8 *(0.59)*	3.1 *(2.2)*	2.6 *(1.2)*
RA25	– *(0.69)*	– –	1.8 *(0.55)*	– –	1.4 *(0.30)*	2.0 *(0.47)*	2.3 *(0.53)*

* The data for TEMPOL are shown in brackets.

From the comparison of data for neutral (TRITON X-100) and zwitterionic (HPS) micelles it follows that the electrostatic effect is small for zwitterionic micelles as well (ΔpK_e values are small). This implies a small influence of the charges in these micelles upon the position of DIPD as compared with the neutral TRITON X-100.

For cationic CTAC micelles the absolute values of ΔpK_e and the electric potential follow the sequence: DIP≈ RA14>RA47>RA25. The relatively high ΔpK_e values for DIP, RA14 and RA47 mean that in the cationic micelles they are localized in a region depleted in protons as compared to the bulk aqueous solution, in other words, close to the positively charged layer of the micelle. The proton concentration in the RA25 environment is closer to the bulk one.

In the case of anionic SDS micelles ΔpK_e shows that RA25 has the closest location to the negatively charged layer of the micelle.

Fluorescence lifetimes and quenching

The decay of the DIPD fluorescence in aqueous homogeneous solutions and in the presence of micelles is biexponential, probably due to the equilibrium between the protonated and neutral species. Data for the lifetimes (Table II) are the average values obtained from the expression (Lakowicz, 1983):

$$\langle\tau\rangle = (\alpha_1\tau_1^2 + \alpha_2\tau_2^2) / (\alpha_1\tau_1 + \alpha_2\tau_2)$$

The bimolecular fluorescence quenching constants (Table V) calculated from the K_{sv} values in aqueous (TEMPOL) and ethanolic (TEMPO) solutions for all DIPD are near the diffusion limit.

In micellar solutions, k_q for TEMPOL is near the diffusion limit of the dynamic quenching for all DIPD in all types of micelles, while k_q for TEMPO is several times greater. The association constant of TEMPO with lysolecithin micelles is higher than 3000 M^{-1} (Tabak and Borissevitch, 1992). TEMPOL has a lower affinity to the micelle and its concentration in the micelle is lower. Since TEMPO molecules have a high affinity to the micelle and are localized preferably inside (Ramachandran *et al.*, 1982), their virtual concentration in micelles is significantly higher than their average bulk concentration. More effective quenching of DIPD fluorescence by TEMPO confirms that all DIPD are bound to the micelles.

^1H NMR spectra

^1H NMR spectra of DIPD are due to the protons of the substituents (Imasato *et al.*, 1993). In order to facilitate data analysis, the spectra of different DIPD are presented and discussed separately.

RA25

For the simplest DIPD, RA25, the spectrum consists of two amine quartets and two methyl doublets corresponding to the substituents in 4-(8-) and 2-(6-) positions of the molecule (Figs.4a, 5a). The spectra are quite similar in $CDCl_3$, DMSO and CCl_4. Upon addition of D_2O to the $CDCl_3$ solution the amine quartets vanish and the methyl doublets broaden due to the exchange of

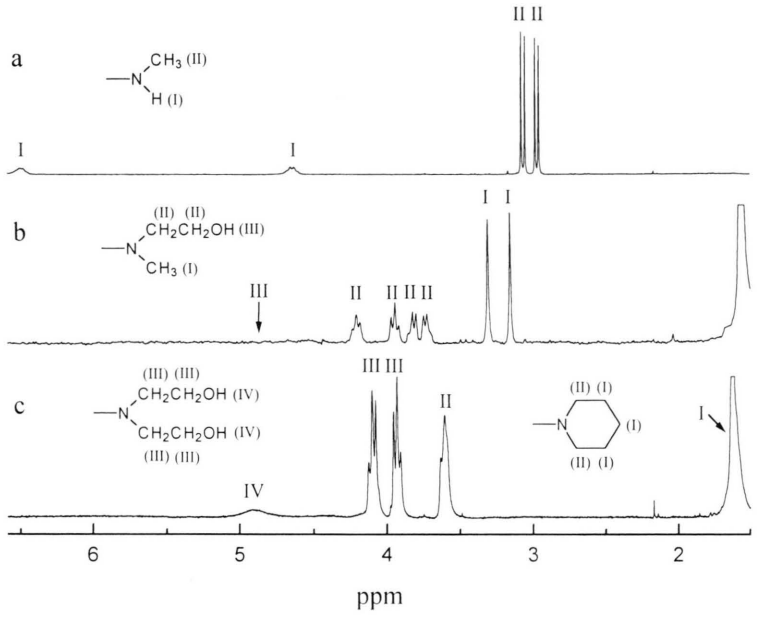

Fig. 4. ^{1}H NMR spectra of RA25 (a), RA47 (b) and RA14 (c) in $CDCl_3$. Concentrations are 1 mM.

the amine protons with those of H_2O (Fig.5b). In H_2O/D_2O solutions two singlet methyl peaks are observed (Fig.5e). They are displaced to higher fields when pH decreases (Fig.6a) suggesting a reduction of electron density probably due to the protonation of the amine nitrogens.

The RA25 spectrum in SDS is similar to that in aqueous solutions (Fig.5d) in the pH region from 1.0 to 10.0. However, in SDS the absolute values of the chemical shifts are equal to those obtained in aqueous solution at pH values higher by 4–5 units (Fig 6b). This result is in reasonable agreement with the ΔpK_a value for RA25 in the SDS micelles (Table III). It may be rationalized in terms of the location of its side substituents in the region of the micelle, where the proton concentration is 4–5 orders of magnitude higher than in the aqueous solution at the same pH, i.e., close to the negatively charged head groups of SDS. In CTAC micelles the spectrum is similar to that in chloroform enriched with water (Fig.5c), in other words, the substituents are located in the region (b) near the external part.

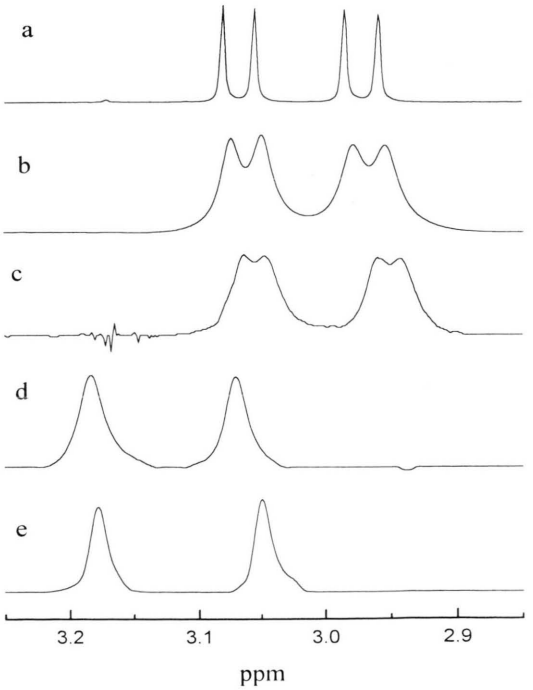

Fig. 5. ^{1}H NMR spectra of the methyl protons of RA25 in $CDCl_3$ (a), $CDCl_3$ + D_2O (b), CTAC (c) and SDS (d) micellar solutions at pH 7.0 and D_2O at pH 3.5 (e). Concentration of RA25 is 1 mM (a,b), 0.5 mM (c,d) and 0.2 mM (e). Concentrations of CTAC and SDS are 80 mM and 50 mM, respectively. The spectrum (c) was obtained by subtraction of the strong micelle peak from the total spectrum.

RA47

The RA47 spectrum in $CDCl_3$ consists of two sets of two triplets (four triplets in total) due to two A_2B_2 systems of the methylene protons of the

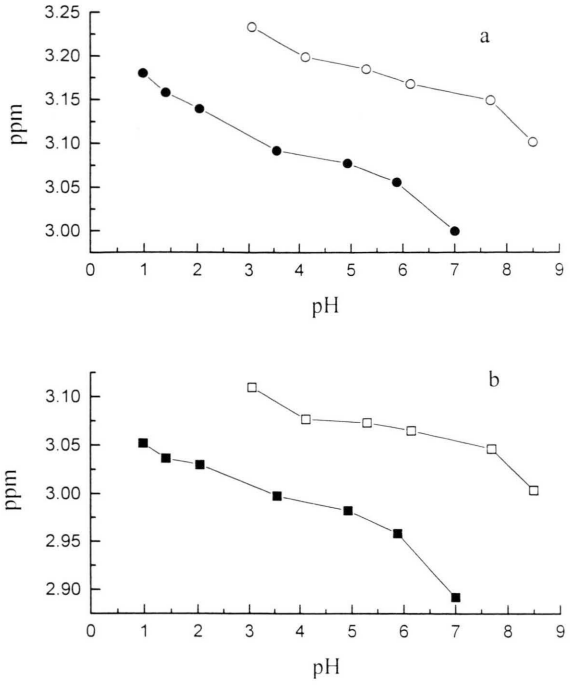

Fig. 6. The position of RA25 methyl ^{1}H NMR peaks (chemical shifts in ppm) in dependence on pH in $H_2O:D_2O = 9:1$ (open symbols) and SDS micellar solution (closed symbols). Concentration of RA25 is 0.2 mM, concentration of SDS is 50 mM. Plots (a) and (b) correspond to high-frequency and low-frequency peaks, respectively.

substituents in the 4-(8-) and 2-(6-) positions, and two singlet peaks of methyl groups (Fig.4b, 7a). In $CDCl_3$ containing considerable amounts of water, the signal from OH groups broadens and practically disappears due to the exchange with water. In aqueous solution the methylene peaks collapse into two unresolved envelopes at 4.02 and 3.87 ppm (Fig.7b).

For RA47 in micelles, the methylene set in the region of 3.9–3.8 ppm (the other set is hidden by the strong micelle peak) for both neutral and protonated drug is similar to that in aqueous solutions (Fig.7c,d). In the spectrum of the neutral form in SDS both methyl peaks are broadened as compared with the aqueous solutions (Fig.7d). For the protonated form, one of the methyl peaks is broadened even more than for the non-protonated one, and the other remains narrow, as in pure water (Fig.7c). This result allows us to assume that the methyl groups of the substituents in protonated RA47 in 4-(8-) and 2-(6-) positions have different surroundings. The protonated RA47 molecules are drawn closer to the micelle surface due to the electrostatic interaction with the SDS micelle charged surface, and hence one pair of the substituents appears in the water phase, probably, in the region (c). Since the subsituents, comprising the pair, have a symmetrical location in the molecule, this could be an additional argument in favor of the parallel orientation of the heterocycle relative to the micelle surface.

Taking into account optical absorption and fluorescence spectra, we can assure that the neutral RA47 molecules are localized in the polar part of the micelles. The molecules of this protonated drug are located in SDS micelles so that two substituents appear in the superficial part of the micelle.

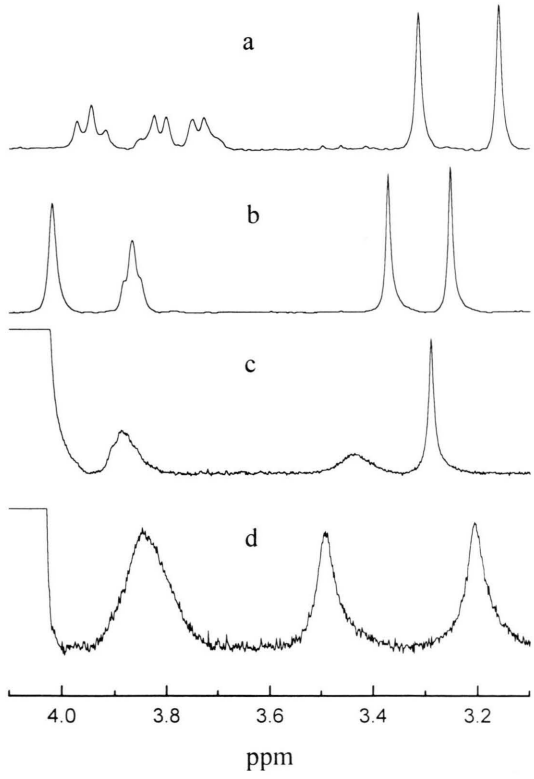

Fig. 7. ^{1}H NMR spectra of RA47 in $CDCl_3$ (a), D_2O (b) and SDS micellar solutions at pH 5.0 (c) and pH 10.0 (d). Concentration of RA47 is 1.0 mM (a) and 0.3 mM (b, c and d), concentration of SDS is 100 mM.

RA14

The RA14 spectrum in $CDCl_3$ (Fig.4c, 8a) consists of one single broadened peak at about 4.9 ppm due to the hydroxyl groups and three triplets which correspond to 3 methylene groups. Two of them, in the 4.2–3.8 ppm region, can be identified as belonging to the ethanolamine substituents due to the A_2B_2 pattern, and the third one at 3.7–3.5 ppm corresponds to the methylenes of the piperidine rings which are close to the nitrogen atoms. The remaining $-CH_2-$ groups of the piperidine rings give a signal at about 1.6–1.7 ppm similar to DIP (Borissevitch *et al.*, 1995); this signal is hidden by the residual water signal and will not be considered further. In aqueous solution two ethanolamine triplets collapse into an unresolved envelope (4.1–3.9 ppm), while the peak of the methylenes of piperidine rings is practically the same as in $CDCl_3$ (Fig.8d). The signals of the ethanolamine protons in CCl_4 consist of three unresolved peaks. The positions of the two external (at the highest and the lowest fields) peaks are practically the same as in $CDCl_3$ and the central one is shifted to high field (Fig.8b).

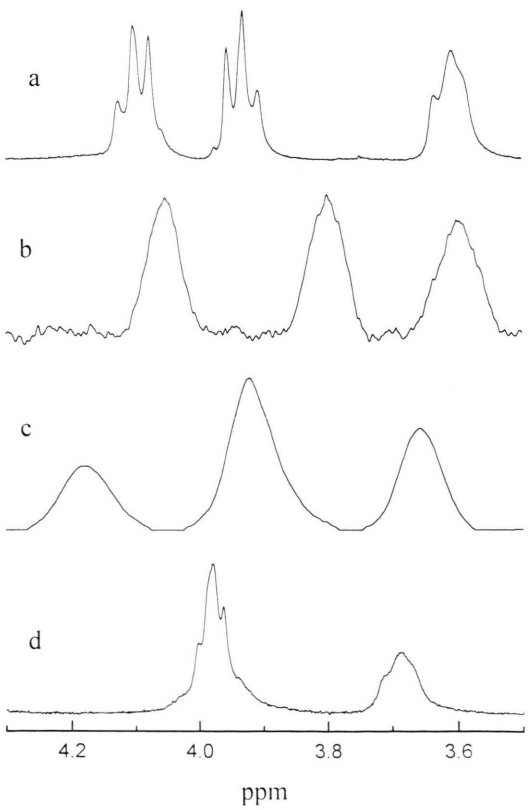

Fig. 8. ^1H NMR spectra of RA14 in $CDCl_3$ (a), CCl_4 (b), CTAC micellar solution at pH 2.0 (c) and D_2O at pH 5.0 (d). Concentration of RA14 is 1 mM (a), <10μM (b) and 0.3 mM (c,d). Concentration of CTAC is 40 mM.

The relative position of the peaks of the RA14 neutral form in the presence of CTAC or SDS is similar to that in nonpolar CCl_4, the spectrum in the whole being shifted to the low field (Fig.8c).

Taken together, the optical and NMR spectral data lead to the conclusion that, similar to DIP (Borissevitch *et al.*, 1995), neutral RA14 molecules are localized in the micelle interior at the "border" of the polar and nonpolar regions so that the heteroaromatic cycle is placed close to this border and the substituents are located in the nonpolar part.

The location in micelles and biological activity

Based on our data, we can assert that despite the difference in structures of the surfactant molecules which determines the architecture of the micelles the main features of DIPD interaction with all types of used micelles are similar.

The structure and the position of the substituents in DIPD affect their binding characteristics and location sites in micelles due to the change of hydrophobicity. Neutral DIP has the highest hydrophobicity and is localized in micelles near the border between the polar (b) and nonpolar (a) regions, having its polarizable heteroaromatic cycle in the region (b) and the nonpolar substituents penetrating into the region (a) of the micelle (Borissevitch *et al.*, 1995). Neutral RA14 molecules with the same substituents in crossed positions possess a hydrophobicity somewhat lower than DIP and have practically the same location in micelles. Neutral RA47 molecules have a hydrophobicity lower than DIP and RA14 and are localized closer to the micelle surface. The heteroaromatic cycle and the substituents in RA47 are positioned in the micellar region (b). Neutral RA25 molecules have the lowest hydrophobicity. They are located near the micelle surface in the region (c) which consists of structurized water molecules. As all DIPD are symmetrical, we can suppose the parallel location of their heterocycles relative to the micelle surface.

High hydrophobicity of neutral DIPD forms is consistent with their low water solubility at physi-

ological pH. This provides their high K_b values upon interaction with micelles.

Protonation of DIPD reduces their K_b for cationic, zwitterionic and neutral micelles and increases it for anionic ones. Electrostatic interaction of the protonated DIPD molecules with the surface charges either moves DIPD into the interior for cationic micelles or draws them closer to the surface for anionic ones. In the case of the protonated RA47 in SDS solution this results in the penetration of two cross substituents into the aqueous phase.

Since their pK_a values are shifted towards lower pH in positive, zwitterionic and neutral micelles, at physiological pHs the DIPD molecules in these micelles are neutral and tightly bound. For anionic micelles the pK_a shift is in the opposite direction. The DIPD molecules are protonated at physiological pHs and also strongly bound. So, at physiological pHs DIPD have high association constants with all types of micelles. This makes it possible to suppose that they are bound effectivelly by membranes *in vivo*.

Hence, we can assume that the presence of the polarizable heterocycle in the structure of a bioactive molecule is necessary to provide its affinity to the polar region of the membrane. The molecules, which have the substituents with relatively low hydrophobicity, are displaced to the membrane surface and the substituents appear in the water phase. The molecules with highly hydrophobic substituents are localized near the border between the polar and the nonpolar region of the membrane and the nonpolar substituents permeate into the hydrophobic membrane interior.

The biological activity of DIPD determined through inhibition of the phosphate or adenosine transport across the membranes of red blood cells (Table III) decreases in accordance with the sequence DIP≈RA14>RA47>RA25 (Von Gerlach *et al.*, 1965). The same sequence describes the depth of DIPD location in the micelles. So, the deeper penetration of DIP and RA14 into the membrane interior could be responsible for their higher activity in these processes as compared with RA47 and RA25 which are located more superficially. We believe that their different location in the membrane should be taken into account while explaining the difference in their biological activity.

Acknowledgments

The authors are indebted to CNP_q, FINEP and FAPESP Brazilian agencies for partial financial support. G.P.Borissevitch, I.E.Borissevitch and V.E.Yushmanov are recipients of visiting grants from CNP_q. We are grateful to Dr. Sylvana C.M.Agostinho for expert technical assistance in NMR spectra measurements. We are also indebted to Dr. Hidetake Imasato for measurements and preliminary analysis of NMR spectra of DIPD in $CDCl_3$.

Alper H.E., Bassolino-Klimas D.and Stouch T.R. (1993), The limiting behavior of water hydrating a phospholipid monolayer: a computer simulation study. J. Chem. Phys. **99,** 5547–5559.

Asoh K.-i., Saburi Y., Sato S.-i., Nogae I., Kohno K., and Kuwano M., (1989), Potentiation of some anticancer agents by dipyridamole against drug-sensitive and drug-resistant cancer cell lines. Jpn. J. Cancer Res. **80,** 475–481.

Batisda E., del Prado J., Almirall L., Janieson G.A. and Ordinas A. (1985), Inhibitory effects of dipyridamole on growth, nucleoside incorporation and platelet-activating capability in the U87G and KNMC human tumor cell lines. Cancer Res. **45,** 4048–4052.

Borges C.P.F. and Tabak M. (1994), Spectroscopic studies of dipyridamole derivatives in homogeneous solutions: effects of solution composition on the electronic absorption and emission. Spectrochim. Acta **50A,** 1047–1056.

Borges C.P.F., Borissevitch I.E. and Tabak M. (1995), Charge- and pH-dependent binding sites of dipyridamole in ionic micelles: a fluorescence study. J. Luminescence **65,** 105–112.

Borissevitch I.E. and Tabak M. (1992), Electronic absorption and fluorescence spectroscopic studies of dipyridamole. Effects of solution composition. J. Luminescence **51,** 315–322.

Borissevitch I.E., Borges C.P.F., Yushmanov V.E. and Tabak M. (1995), Localization of dipyridamole molecules in ionic micelles: effect of micelle and drug charges. Biochim. Biophys. Acta **1238,** 57–62.

Borissevitch G., Tabak M. and Oliveira Jr. O. N. de (1996), Interaction of dipyridamole with lipids in mixed Langmuir monolayers. Biochim. Biophys. Acta **1278,** 12–18.

Chen H.-X., Bamberger U., Heckel A., Guo X. and Cheng Y.-C. (1993), BIBW 22, a dipyridamole analogue, acts as a bifunctional modulator on tumor cells by influencing both P-glycoprotein and nucleoside transport. Cancer Res. **53,** 1974- 1977.

Davies J.T. and Rideal E.K. (1961), Interfacial phenomena, Academic Press, Inc.

Drummond C.J., Grieser F. and Healy T.W. (1988), Interfacial properties of a novel group of solvatochromic acid-base indicators in self-assembled surfactant aggregates. J. Phys. Chem. **92,** 2604–2613.

Fernández M.S. and Fromherz P. (1977), Lipoid pH indicators as probes of electrical potential and polarity in micelles. J. Phys. Chem. **81,** 1755–1761.

Ford J.M. and Hait W.N. (1990), Pharmacology of drugs that alter multidrug resistance in cancer. Pharmacological Reviews **42,** 155–199 and references therein.

Ganesh K.N., Mitra P. and Balasubramanlan D. (1982), Solubilization sites of aromatic optical probes in micelles. J. Phys. Chem. **86,** 4291–4293.

Hiramatsu M., Kadowaki D., Edamatsu R., Liu J., Wang X., Ohba S., and Mori A., (1992), Antioxidant action of dipyridamole. In: Guanidino compounds in biology and medicine (eds. by P.P.De Deyn, B.Marescau, V.Stalon and I.A.Qureshi, John Libbey & Company Ltd.), 425–432.

Imasato H., Borges C.P.F., Yushmanov V.E., Perussi J.R. and Tabak M. (1993), ^{1}H and ^{13}C NMR of dipyridamole derivatives in homogeneous solution: correlation to the electron density. In: Anais de IV encontro de usuários de resonância magnética nuclear, Rio de Janeiro, 437–442.

Iuliano L., Violi F., Ghiselli A., Alessandri C. and Balsano F. (1989), Dipyridamole inhibits lipid peroxidation and scavenges oxygen free radicals. Lipids **24,** 430- 433.

Iuliano L., Praticò D., Ghiselli A., Bonavita M.S. and Violi F. (1992), Reaction of dipyridamole with the hydroxyl radical. Lipids **27,** 349–353.

Iuliano L., Pedersen J.Z., Rotilio G., Ferro D. and Violi F. (1995), A potent chain- breaking antioxidant activity of the cardiovascular drug dipyridamole. Free Radic. Biol. Med. **18,** 239–247.

Kaneshina S, Kamaya H. and Ueda I. (1984), Benzyl alcohol penetration into micelles, dielectric constants of the binding site, partition coefficients and high-pressure squeeze-out. Biochim. Biophys. Acta **777,** 75–83.

Lakowicz J.R. (1983), Principles of fluorescence spectroscopy, Plenum Press.

Lee A.G. (1978), Effects of charged drugs on the phase transition temteratures of phospholipid bilayers. Biochim. Biophys. Acta **514,** 95–104.

Louro S.R.W., Nascimento O.R. and Tabak M. (1994), Charge- and pH-dependent binding sites for dibucaine in ionic micelles: a fluorescence study. Biochim. Biophys. Acta **1190,** 319–328.

Marchandt E., Prichard A.D., Casanegra P. and Lindsay L. (1984), Effect of intravenous dipyridamole on regional coronary blood flow with 1-vessel coronary artery disease: evidence against coronary steal. Amer. J. Cardiology **53,** 718–721.

Marshall R.J. and Parrat J.R. (1973), The effects of dipyridamole on blood flow and oxygen handling on the acutely oschaemic and normal canine myocardium. Br. J. Pharmacol. **49,** 391–399.

Oliveira O.N. Jr., Taylor D.M., Lewis T.J., Salvagno S. and Stirling C.J.M. (1989), Estimation of group dipole moments from surface potential measurements on langmuir monolayers. J. Chem. Soc., Faraday Trans. 1 **85,** 1009–1018.

Ramachandran C., Pyter R.A. and Mukerjee P. (1982), Microenvironmental effects on energies of visible bands of nitroxides in electrolyte solution and when solubilized in micelles of different charge types. Significance of effective polarity estimates. implications for spectroscopic probe studies in lipid assemblies. J. Phys. Chem. **86,** 3198–3205.

Ramu N. and Ramu A. (1989),Circumvention of adriamycin resistance by dipyridamole analogues: a structure-activity relationship study. Int. J. Cancer **43,** 487–491.

Rooney E.K., East J.M., Jones O.T., McWhirter J., Simmonds A.S. and Lee A.G. (1983), Interaction of fatty acids with lipid bilayers. Biochim. Biophys. Acta **728,** 159–170.

Shalinsky D.R., Andreeff M. and Howell S.B. (1990), Modulation of drug – sensitivity by dipyridamole in multidrug resistant tumor cells in vitro. Cancer Res. **50,** 7537–7543.

Shalinsky D.R., Jekunen A.P., Alcaraz J.E., Christen R.D., Kim S., Khatibi S. and Howell S.B. (1993), Regulation of initial vinblastine influx by P-glycoprotein. Br. J. Cancer **67,** 30–36.

Tabak M. and Borissevitch I.E. (1992), Interaction of dipyridamole with micelles of lysophosphatidylcholine and with bovine serum albumin: fluorescence studies. Biochim. Biophys. Acta **1116,** 241–249.

Tanford C. (1973), The hydrophobic effect: formation of micelles and biological membranes. John Wiley & Sons, New York, London, Sydney, Toronto.

Taylor D.M., de Oliveira O.N. Jr. and Morgan H. (1990), Models for interpreting surface potential measurements and their application to phospholipid monolayers. J. Colloid Int. Sci. **139,** 508–518.

Thomas J.K. (1980), Radiation-induced reactions in organized assemblies. Chem.Rev. **80,** 283–299.

Tocanne J.F. and Teissié J. (1990), Ionization of phospholipids and phospholipid- supported interfacial lateral diffusion of protons in membrane model systems. Biochim. Biophys. Acta **1031,** 111–142.

Von Gerlach E., Deuticke B. and Koss F.W. (1965), Einfluß von Pyrimidopyrimidin- und pteridin-derivaten auf Phosphat- und Adenosinpermeabilität menschlicher Erythrocyten (influence of derivatives of pyrimido-pyrimidine and pteridine on phosphate and adenosine permeability of human erythrocytes.) Arzneim. Forsch. (Drug Research) **15,** 558–563.

Wennerström H. and Lindman B. (1979), Water penetration into surfactant micelles. J. Phys. Chem. **83,** 2931–2932.

Zhen Y., Taniki T. and Weber G. (1992), Azidothymidine and dipyridamole as biochemical response modifiers: synergism with methotrexate and 5-fluorouracil in human colon and pancreatic carcinoma cells. Oncology Res. **4,** 73–78.